Modeling speleothem $\delta^{13}C$ variability in a central Sierra Nevada cave using ^{14}C and $^{87}Sr/^{86}Sr$

Jessica L. Oster [a,*], Isabel P. Montañez [a], Thomas P. Guilderson [b,d], Warren D. Sharp [c], Jay L. Banner [e]

[a] Geology Department, University of California, Davis, USA
[b] Center for AMS, Lawrence Livermore National Lab, Livermore, CA, USA
[c] Berkeley Geochronology Center, Berkeley, CA, USA
[d] Institute of Marine Sciences, University of California – Santa Cruz, USA
[e] University of Texas, Austin, USA

Abstract

Carbon isotopes in speleothems can vary in response to a number of complex processes active in cave systems that are both directly and indirectly related to climate. Progressing downward from the soil zone overlying the cave, these processes include soil respiration, fluid–rock interaction in the host limestone, degassing of CO_2 and precipitation of calcite upflow from the speleothem drip site, and calcite precipitation at the drip site. Here we develop a new approach to independently constrain the roles of water–rock interaction and soil processes in controlling stalagmite $\delta^{13}C$. This approach uses the dead carbon proportion (dcp) estimated from coupled ^{14}C and $^{230}Th/U$ measurements, in conjunction with Sr isotope analyses on stalagmite calcite from a central Sierra Nevada foothills cave in California, a region characterized by a highly seasonal Mediterranean-type climate, to determine the roles of water–rock interaction and soil processes in determining stalagmite $\delta^{13}C$. Increases in stalagmite dcp between 16.5 and 8.8 ka are coincident with decreased $\delta^{13}C$, indicating a varying yet substantial contribution from the soil organic matter (SOM) reservoir, likely due to significantly increased average age of SOM in the soil veneer above the cave during wet climatic intervals.

We use geochemical and isotope mixing models to estimate the host-carbonate contribution throughout the $\delta^{13}C$ time series and determine the degree of degassing and calcite precipitation that occurred prior to precipitation of stalagmite calcite. The degree of degassing and prior calcite precipitation we calculate varies systematically with other climate indicators, with less degassing and prior calcite precipitation occurring during wetter climatic intervals and more during drier intervals. Modeled $\delta^{13}C$ values and degassing calculations suggest that some degree of prior calcite precipitation is necessary at all time intervals to explain measured stalagmite $\delta^{13}C$ values, even during relatively wet intervals. These results illustrate the importance of constraining degassing and prior calcite precipitation in the interpretation of speleothem $\delta^{13}C$ records, particularly those from caves that formed in seasonal semi-arid to arid environments.
© 2010 Elsevier Ltd. All rights reserved.

1. INTRODUCTION

Speleothems, or secondary cave precipitates, provide archives of paleoenvironmental change in the terrestrial environments where humans evolved and currently live and raise food (McDermott, 2004). The majority of speleothem-based paleoclimate studies have focused on speleothem $\delta^{18}O$ records as proxies of variability in the isotopic composition of rainfall (e.g., Wang et al., 2001, 2005; Partin et al., 2007; Cruz et al., 2009; Cheng et al., 2009; Wagner et al., 2010; Asmerom et al., 2010). However, many other proxies can shed light on regional climate variability, including $\delta^{13}C$ (Dorale et al., 1998; Genty et al., 2003; Cruz

et al., 2006), trace element concentrations (Treble et al., 2005; Johnson et al., 2006; Oster et al., 2009), strontium isotopes (Banner et al., 1996; Oster et al., 2009), and growth rates (Baker et al., 1998; Polyak et al., 2004; Ersek et al., 2009). Whereas multi-proxy studies allow the investigation of a range of environmental processes, including climatically driven water–soil–rock interactions and shifts in vegetation, they can also highlight the complexity and variability of cave systems. For example, changes in the degree of open versus closed-system dissolution or local hydrology in a cave system may confound or mask the influence of climate change on speleothem proxy records (Hendy, 1971; Genty et al., 2001; Oster et al., 2009). Speleothem $\delta^{13}C$ variations in particular can be challenging to interpret given the wide range of processes that can influence speleothem $\delta^{13}C$ values. These include: (1) the ratio of C_3 to C_4 plant species above a cave (Dorale et al., 1998), (2) the rate of soil respiration and the relative contribution to dissolved inorganic carbon of soil-respired CO_2 versus atmospheric CO_2 (Genty et al., 2001, 2003), (3) kinetically induced isotopic disequilibrium during calcite precipitation (Hendy, 1971; Mickler et al., 2004), (4) the extent of fluid–rock interaction (Hendy, 1971; Genty et al., 2001), and (5) degassing of CO_2 and precipitation of calcite upflow from the speleothem drip site (Baker et al., 1997; Mickler et al., 2004; Fairchild, 2006).

Previously, we showed that variations in $\delta^{13}C$ along with $\delta^{18}O$, $^{87}Sr/^{86}Sr$, and [Sr], [Mg], and [Ba] in a stalagmite from a central Sierra Nevada foothill cave (Moaning Cave, CA, Fig. 1) primarily reflect changes in precipitation amount during the past deglacial (16.5–8.8 ka) (Oster et al., 2009). The Moaning Cave stalagmite proxies record drier and possibly warmer conditions, signified by elevated

$\delta^{13}C$, $\delta^{18}O$, trace element contents, and $^{87}Sr/^{86}Sr$ values, during Northern Hemisphere warm periods (Bølling, early and late Allerød) and wetter and possibly colder conditions indicated by decreased $\delta^{13}C$, $\delta^{18}O$, and trace element contents and less radiogenic $^{87}Sr/^{86}Sr$ during Northern Hemisphere cold periods (Older Dryas, Inter-Allerød Cold Period, and Younger Dryas).

Here we use geochemical modeling and ^{14}C, $^{87}Sr/^{86}Sr$, and $\delta^{13}C$ measurements from the same Moaning Cave stalagmite (MC3) to illustrate how dead carbon proportion (dcp) and $^{87}Sr/^{86}Sr$ ratios provide independent constraints on the origin of $\delta^{13}C$ variability previously documented (Oster et al., 2009). Our results illustrate how the integrated use of ^{14}C, $^{87}Sr/^{86}Sr$, and geochemical modeling, for a given cave system, further constrains: (1) the degree of interaction of vadose waters with the carbonate host to the cave, (2) the extent of CO_2 degassing and prior calcite precipitation along the vadose-water flow path to the drip site, and (3) the influence of the soil carbon reservoir on speleothem $\delta^{13}C$ variability. These processes are three of the primary influences on stalagmite carbon isotope values in karst systems and are closely tied to climate variability, in particular in temperate, semi-arid climates where drip rates can have substantial seasonal variability. Caves in these regions are relatively poorly understood compared to caves from tropical and subtropical environments where surface humidity and cave drip rates are less variable.

2. SITE AND SAMPLE DESCRIPTION

Moaning Cave (Fig. 1) is a vertical solution cavity and dome pit developed along vertical fractures within one of several discrete carbonate masses in the Sierra Nevada
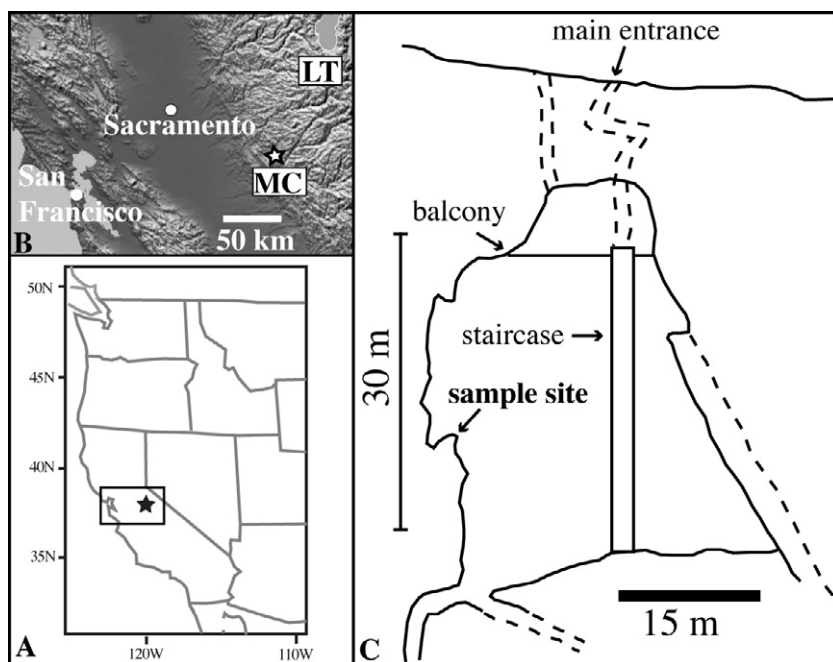

Fig. 1. (A) Location of Moaning Cave (MC: 38.07°N, 120.47°W, 520 m a.s.l.) in western North America. (B). Relief map of east–west transect across north Central Valley Region, California. MC, Moaning Cave; LT, Lake Tahoe. (C) Cross-section through a portion of Moaning Cave showing location of sample collection (after Short, 1975).

foothills (Clark and Lydon, 1962; Bowen, 1973; Short, 1975). The carbonate consists of lenticular masses of metamorphosed Permo-Carboniferous limestone and dolomite tectonically interleaved with other metasedimentary and metavolcanic rocks of the Calaveras Complex. Moaning Cave is developed in the Columbia carbonate mass, which is oriented NE–SW and is 6.5 km long by 2.4–4 km wide (Clark and Lydon, 1962). The cave has two natural entrances at 520 m above sea level situated above a large >37 m tall room. Additional rooms extend 64 m below the main room (Short, 1975).

The climate above Moaning Cave is characterized by cool, wet winters and hot, dry summers. Jamestown, California, a town 13 km to the southeast of Moaning Cave (550 m elevation), experienced an average yearly rainfall of ~430 mm between March 2006 and July 2009. Approximately 88% of yearly precipitation falls between October and April when the polar jet stream migrates southward bringing winter storms from the North Pacific into the region. Railroad Flat, a higher elevation site (800 m) 26 km to the north of Moaning Cave with longer-duration monitoring (1989–present), experiences a similar yearly distribution (76% rainfall occurs during the winter months), but higher annual rainfall (820 mm/year). The soil above Moaning Cave is a moderately drained inceptisol resting on fractured marble that ranges from a few centimeters to half a meter in thickness. Present vegetation above the cave consists of C_3 plants, including manzanita (*Arctostaphylos* sp.), toyon (*Heteromeles arbutifolia*), and other chaparral species.

Five 2.5 cm diameter cores (Fig. 2) were drilled through (MC3-A) and around (MC3-B through E) the modern drip center of a meter-wide stalagmite (MC3) in order to capture movement of the drip center through time. MC3, which is fed by a fracture in the cave ceiling ~12 m above, is 1.5 m tall along the central axis and sits on a slope 30 m vertically below the cave entrance. At the sample location, rock thickness above the cave is ~15 m. A HOBO® data logger left at the MC3 sample site between August 2005 and August 2007

documents temperature and humidity variations from 15.2 to 17.5 °C and 90% to 100%, respectively, throughout the year. Natural drip-water flow within the cave increases substantially during the winter season (up to 60 drips/m) and almost entirely ceases (1–2 drips/m) during the summer.

3. METHODS

3.1. U-series

Four samples for U–Th dating were drilled from MC3-A following visible growth bands. Five additional samples were sawed from MC3-B, C, and D. The locations of samples from these cores were correlated to MC3-A by visually matching growth bands and $\delta^{18}O$ and $\delta^{13}C$ series among the cores (Oster et al., 2009).

Chemical separation of U and Th was carried out according to procedures described in Edwards et al. (1987). Isotopic analyses were performed at the Berkeley Geochronology Center on a Micromass Sector-54 TIMS equipped with a wide-angle, retarding-potential energy filter and Daly-type ion counter. Mass discrimination for U was corrected using the known $^{233}U/^{236}U$ ratio of the spike, whereas thorium ratios were uncorrected. The U–Th spike was calibrated against solutions of HU-1 (Harwell uraninite) standard and solutions of 69 Ma uranium ore from the Schwartzwalder Mine that have been demonstrated to yield concordant U/Pb ages (Ludwig et al., 1985) and sample-to-sample agreement of $^{234}U/^{238}U$ and $^{230}Th/^{238}U$ ratios. Instrumental performance was monitored by frequent analyses of the Schwartzwalder Mine secular equilibrium standard. Procedural backgrounds for $m/e = 230$ averaged <0.6 femtogram ^{230}Th equivalent, and were negligible for ^{238}U and ^{232}Th. Ages were determined using the decay constants of Cheng et al. (2000). Ages and errors were calculated using Isoplot (Ludwig, 2003).

3.2. Stable isotope compositions

Stable isotope samples (25–75 μg) were microdrilled from thick sections along the growth axis of the Moaning Cave core using an automated Merchantek microdrilling system with ~50 μm spatial resolution providing decadal to centennial temporal resolution. Stable isotope samples were roasted at 375 °C *in vacuo* to eliminate organic volatiles and fluid inclusions (Sarkar et al., 1990). $\delta^{13}C$ values were determined using a Fisons Optima IRMS with a 90 °C Isocarb common acid bath autocarbonate system in the Department of Geology stable isotope laboratory at UC Davis. Values are reported relative to Vienna Pee Dee Belemnite (V-PDB) using standard delta notation; long-term analytical precision for $\delta^{13}C$ is ~±0.1‰ (2σ) based on repeat analysis of an in-house carerra marble standard. $\delta^{13}C$ profiles were also completed for dated intervals of cores MC3-B and MC3-C.

3.3. Strontium isotopes

Calcite from the speleothem, microsampled at a 1 mm intervals, and six samples of host carbonate were processed
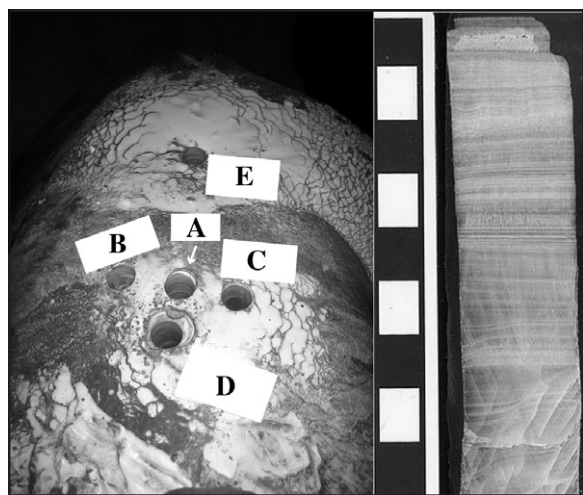

Fig. 2. Photograph of MC3 stalagmite with locations of cores A–E. Cores are 1 in. in diameter. Photograph of top 9 cm of core MC3-A. Scale bar increments in cm.

for Sr isotope analysis using chemical pre-treatments to remove Sr associated with absorbed or included non-carbonate phases (Montañez et al., 2000). Seven soil samples from the area immediately above Moaning Cave were leached with progressively stronger solutions (1 M ammonium acetate, 4% acetic acid, concentrated (48 M) hydrofluoric acid) in order to characterize the $^{87}Sr/^{86}Sr$ ratio of leachable Sr in soil components (carbonate, volcanic grains, and phyllosilicates). In addition, four samples of metamorphic rocks (metamorphosed ash, basalt, and amphibolite) that occur in the vicinity of Moaning Cave were fully dissolved in order to determine their $^{87}Sr/^{86}Sr$ value. For all rock samples and leachates, strontium was isolated using Spex cation exchange resin. $^{87}Sr/^{86}Sr$ ratios were measured in solution mode on a Nu MC-ICPMS in the Geology Department at UC Davis and values were normalized to a nominal value for SRM987 of 0.710248. SRM987 for the measurement period was 0.710147 ($2\sigma = 4.5 \times 10^{-5}$) based on 18 standards analyzed during this period.

3.4. Radiocarbon

Twenty-six samples, $\leqslant 1$ mm in width, were sawed from cores MC3-A, B, and C for radiocarbon analysis, providing a temporal resolution of 50–300 years. Coarsely crushed subsamples ($\sim$12–17 mg) were leached with 0.1 N HCl to remove surface calcite that may have adsorbed atmospheric CO_2, rinsed twice with 18-Ω miliQ water, and dried. Samples were placed in individual reaction vessels, evacuated, heated, and acidified with orthophosphoric acid. The evolved CO_2 was purified, trapped, and converted to graphite in the presence of an iron catalyst in individual reactors in a process similar to that described by Vogel et al. (1987). Graphite targets were measured at the Center for Accelerator Mass Spectrometry at Lawrence Livermore National Laboratory. Analyses are reported as per the convention put forth by Stuiver and Polach (1977) and include a matrix specific background correction using speleothem calcite that was $^{230}Th/U$ dated to 200 ka. Uncertainties are propagated as described in Guilderson et al. (2003).

4. RESULTS

4.1. U-series

U–Th data and ages of the MC3 speleothem were presented in Oster et al. (2009). U concentrations in the MC3 speleothem range from $\sim$130 to 500 ppb (median 456 ppb). Relatively high concentrations of ^{232}Th in the speleothem cores ($\sim$1–15 ppb, median 4.2 ppb) indicate the presence of silicate detritus likely derived from wind blown dust or soil above the cave. As discussed by Hellstrom (2006), limiting values for initial isotopes of U and Th consistent with preservation of stratigraphic order may be derived from a sequence of speleothem samples with varying $^{230}Th/^{232}Th$ ratios. Using this approach, we have corrected for U and Th isotopes contributed by detritus using activity ratios of $(^{232}Th/^{238}U) = 1.45 \pm 0.35$, $(^{230}Th/^{238}U) = 1.0 \pm 0.25$, and $(^{234}U/^{238}U) = 1.0 \pm 0.25$. The uncertainty assigned to the $^{232}Th/^{238}U$ ratio of detritus

delimits the range of that ratio consistent with preservation of stratigraphic order, while the uncertainties assigned to the $^{230}Th/^{238}U$ and $^{234}U/^{238}U$ ratios represent generous estimates of likely uncertainties in those ratios (e.g., Ludwig and Paces, 2002). Uncertainties in the isotope ratios of detritus were propagated through to the ages. Ages are summarized in Table 1, and shown with uncertainties as a stalagmite growth curve in Fig. 3.

4.2. Strontium isotopes

The Moaning Cave host carbonate has a $^{87}Sr/^{86}Sr$ value of 0.70744 ± 0.00036. Soil leachate $^{87}Sr/^{86}Sr$ values are 0.70535 ± 0.0008 for the weak ammonium acetate leaches, 0.7052 ± 0.0013 for the acetic acid leaches, and 0.70412 ± 0.00046 for the HF dissolutions. The overall average for soil leachates is 0.70489 ± 0.0011. The $^{87}Sr/^{86}Sr$ values for Moaning Cave soil leachates that are less radiogenic than the host marble on which the soils are developed, suggest some contribution of Sr to the soil from metamorphic and altered volcanic rocks located above the cave ($^{87}Sr/^{86}Sr = 0.70353 \pm 0.00027$). Speleothem $^{87}Sr/^{86}Sr$ values vary between 0.70577 and 0.70689 (Fig. 4D), falling between values for the soil leachates and the host marble.

4.3. Radiocarbon results and dead carbon calculations

Radiocarbon measurements on the Moaning Cave stalagmite are reported in Table 2 and Fig. 3. Radiocarbon ages were calibrated using the IntCal09 calibration set (Reimer et al., 2010). The calibrated radiocarbon ages are consistently older than the corresponding U-series ages of the Moaning Cave stalagmite (Fig. 3), indicating the presence of carbon depleted in ^{14}C relative to the contemporaneous atmosphere. Such carbon could be derived either by dissolution of the host marble or CO_2 from older soil organic matter, or both. The difference between the U-series and calibrated radiocarbon ages varies with stalagmite age, indicating that the proportion of ^{14}C-depleted carbon also varied from 16 to 8.8 ka.

To provide a quantitative measure of ^{14}C-depleted carbon in the stalagmite, we calculated the dead carbon proportion (dcp) following the methods of Genty and Massault (1999) and Genty et al. (2001):

$$dcp = [1 - (a^{14}C_{init.}/a^{14}C_{atm.init.})] * 100\%, \qquad (1)$$

where $a^{14}C_{atm.init.}$ is the atmospheric ^{14}C activity at the time of calcite deposition, determined using the IntCal09 calibration curve (Reimer et al., 2010) and the U-series age of the speleothem calcite. The $a^{14}C_{init.}$ value is the initial ^{14}C activity of the calcite given by:

$$a^{14}C_{init.} = a^{14}C_{meas.}/(\exp(-\ln(2)/5730) * t), \qquad (2)$$

where t is the U-series age of the calcite in calendar years and $a^{14}C_{meas.}$ is the measured ^{14}C activity of the calcite.

The uncertainties of dcp values were calculated by propagating the 2σ errors reported for the U-series and ^{14}C measurements through the dcp calculation. The larger of the two uncertainties is used. With the exception of the youngest data point, errors on the U-series measurements lead

Table 1
^{230}Th/U analytical data and ages for MC3 speleothem.

Sample	Depth (mm)	Wt (mg)	U (ppm)	^{232}Th (ppm)	^{230}Th/^{232}Th	Measured ^{230}Th/^{238}U	Measured ^{234}U/^{238}U	Uncorrected ^{230}Th Age (ka)	Corrected ^{230}Th Age (ka)	Initial ^{234}U/^{238}U
MC1	9	274.5	0.302	0.00281	28.2	0.08672 ± 0.0011	1.097 ± 0.0034	8.98 ± 0.12	8.77 ± 0.14	1.099 ± 0.003
MC9	18	515.2	0.465	0.00473	26.1	0.08753 ± 0.0009	1.091 ± 0.0065	9.12 ± 0.11	8.89 ± 0.14	1.094 ± 0.007
MC8A(1)	21.3	401.5	0.473	0.00418	34.5	0.1004 ± 0.0016	1.093 ± 0.0026	10.51 ± 0.18	10.31 ± 0.19	1.095 ± 0.003
MC8A(2)	21.3	450.7	0.458	0.00402	34.4	0.09958 ± 0.0014	1.086 ± 0.0048	10.49 ± 0.16	10.29 ± 0.18	1.089 ± 0.005
MC8B	21.3	413.5	0.456	0.00424	33.0	0.1011 ± 0.0022	1.093 ± 0.0052	10.58 ± 0.24	10.37 ± 0.25	1.096 ± 0.005
MC 4-1		436.3	0.463	0.01300	11.7	0.1081 ± 0.0021	1.093 ± 0.0087	11.36 ± 0.25	10.72 ± 0.34	1.096 ± 0.009
MC 4-2		532.8	0.461	0.00664	22.3	0.1059 ± 0.0023	1.092 ± 0.0044	11.12 ± 0.26	10.79 ± 0.28	1.095 ± 0.005
MC5B	22.5	356.5	0.457	0.00733	19.7	0.1042 ± 0.0037	1.069 ± 0.0044	11.19 ± 0.42	10.82 ± 0.44	1.071 ± 0.005
MC3	23	391.8	0.493	0.0108	16.6	0.1198 ± 0.0026	1.094 ± 0.0016	12.64 ± 0.30	12.14 ± 0.35	1.098 ± 0.002
MC5	25	401.9	0.443	0.0158	10.3	0.1208 ± 0.0029	1.068 ± 0.0037	13.09 ± 0.34	12.26 ± 0.45	1.071 ± 0.004
MC10	41	803.5	0.168	0.00164	44.4	0.1425 ± 0.0017	1.098 ± 0.0036	15.14 ± 0.21	14.92 ± 0.22	1.103 ± 0.004
MC 4-4		663.0	0.127	0.00090	65.9	0.1547 ± 0.0016	1.102 ± 0.0064	16.48 ± 0.21	16.32 ± 0.22	1.107 ± 0.007
MC2	67	330.5	0.174	0.00093	88.3	0.1564 ± 0.0030	1.105 ± 0.0025	16.63 ± 0.35	16.51 ± 0.35	1.110 ± 0.003
MC 4-5		473.9	0.146	0.00527	13.6	0.1626 ± 0.0036	1.084 ± 0.0063	17.71 ± 0.44	16.88 ± 0.53	1.089 ± 0.007

All isotope ratios are given as activity ratios; errors are 2σ. Activity ratios used for detritus correction are (^{232}Th/^{238}U), 1.45 ± 0.35; (^{230}Th/^{238}U), 1.0 ± 0.25; (^{234}U/^{238}U), 1.0 ± 0.25. Decay constants used are from Cheng et al. (2000). Initial ^{234}U/^{238}U calculated from present day, detritus-corrected ^{234}U/^{238}U and corrected ^{230}Th age. Samples MC8A(1), MC8A(2), and MC9 were taken from Core MC3-B. Samples MC5B, MC8B, and MC10 were taken from Core MC3-C. Corresponding depths in Core MC3-A are given. Weighted mean age of samples MC8A(1), MC8A(2), and MC8B used for age model is 10.32 ± 0.21 ka. Samples MC 4-1 through MC 4-5, taken from Core MC3-D, are not included in the age model, but were used to determine the (^{232}Th/^{238}U) for detritus correction.
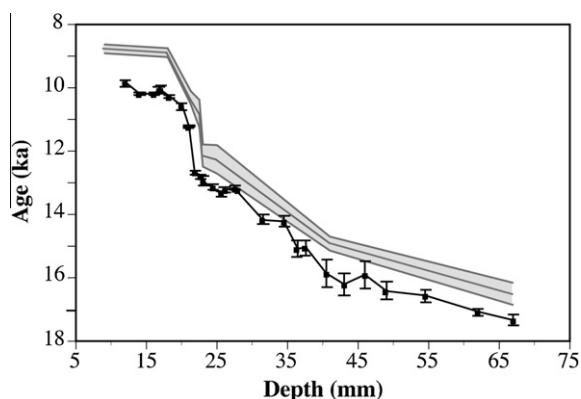

Fig. 3. Comparison of U-series age model (gray) with calibrated ^{14}C ages (black) versus depth for the MC3 stalagmite.

to larger uncertainty in the dcp value than do errors on the radiocarbon measurements.

The calculated dcp of the Moaning Cave stalagmite varies from <1% to ~16% between 8.8 and 16.5 ka (Fig. 4B). The dcp remains relatively low (2–11%) between 16 and 12.4 ka. Earlier than 12.4 ka, peaks in dcp generally coincide with δ^{13}C minima in the Moaning Cave record, though the two records are not correlated ($r^2 = 0.02$). Later than 12.4 ka, dcp is much more variable (0.35–16%), and no clear relationship between dcp and δ^{13}C exists.

5. DISCUSSION

In the following sections, we take a three-step approach to evaluate the sources and processes that influence stalagmite δ^{13}C. These include the contribution of soil organic carbon and host-rock dissolution to seepage-water DIC

and stalagmite δ^{13}C values at Moaning Cave, and the degree to which degassing and prior calcite precipitation in the epikarst are required to account for the variability in the measured δ^{13}C record. In the first step, we use the dcp time series determined for the MC stalagmite to constrain the contribution of soil organic carbon to dissolved inorganic carbon and ultimately to stalagmite δ^{13}C. In the second step, we use geochemical mixing models (Fig. 5) to define a stalagmite δ^{13}C record for which all variability in δ^{13}C is controlled by two carbon end-member sources, i.e., host carbonate and dissolved CO_2 from soil organic material above Moaning Cave. This mixing model does not reproduce observed stalagmite δ^{13}C values and thus documents that plausible variations in the contribution of carbon from these two end-members alone cannot explain the Moaning Cave δ^{13}C record. These results suggest the additional influence of degassing of CO_2 and prior calcite precipitation in the epikarst on stalagmite δ^{13}C. Therefore, in the third step, we use a Rayleigh-type fractionation to constrain the magnitude of the influence of degassing and prior calcite precipitation on the stalagmite δ^{13}C record from Moaning Cave (Mickler et al., 2004).

5.1. Inferring the sources of stalagmite δ^{13}C variation

Measured stalagmite δ^{13}C values for Moaning Cave are more negative (−11.2‰ to −9.5‰) during Northern Hemisphere cold periods (e.g., late glacial, Older Dryas, Inter-Allerød Cold period, Younger Dryas) and less negative (−5.8‰ to −8.0‰) during warm periods (e.g., Bølling, early and late Allerød) (Fig. 4C and F) (Oster et al., 2009). Intervals of lower δ^{13}C coincide with lower stalagmite δ^{18}O (Fig. 4E) increased stalagmite growth rates and calcite textures consistent with precipitation under relatively high and consistent drip rates. These characteristics
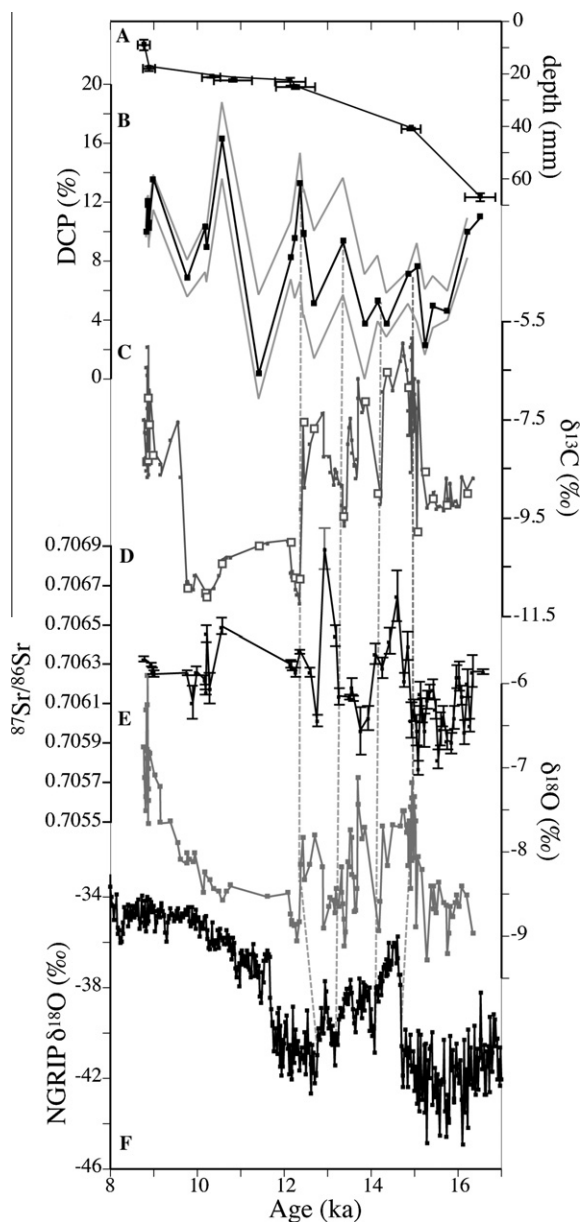
Fig. 4. Comparison of (A) age-depth profile, (B) dead carbon proportion (dcp), measured (C) $\delta^{13}C$, (D) $^{87}Sr/^{86}Sr$, and (E) $\delta^{18}O$ for the MC3 (core A) stalagmite with (F) $\delta^{18}O$ for the NGRIP ice core (Andersen et al., 2005; Svensson et al., 2006). Gray band indicates errors on dcp. White boxes on $\delta^{13}C$ profile correspond to dcp measurements (with the exception of the oldest dcp measurement). Dashed lines tie the onset of the B-A (~14.9 ka) and the YD (~12.4 ka) and the Older-Dryas (~14.1 ka) and Inter-Allerød Cold Period (~13.3 ka) in the MC3 record to the NGRIP ice core record.

are consistent with a wetter climate above Moaning Cave during Northern Hemisphere cold periods. Conversely, Northern Hemisphere warm periods are characterized in the MC3 stalagmite by slower growth rates, microcrystalline calcite fabrics recording intermittent growth, and more positive $\delta^{13}C$ and $\delta^{18}O$ values, which we previously interpreted to reflect drier conditions above the cave (Oster

et al., 2009). Overall, long-term (millennial-scale) trends in stalagmite $\delta^{13}C$ values coincide with variations in stalagmite $^{87}Sr/^{86}Sr$, with less negative $\delta^{13}C$ corresponding with more radiogenic $^{87}Sr/^{86}Sr$ and more negative $\delta^{13}C$ corresponding with less radiogenic $^{87}Sr/^{86}Sr$. However, variations in stalagmite $\delta^{13}C$ and $^{87}Sr/^{86}Sr$ do not coincide at the submillennial-scale (Fig. 4C and D).

Dead carbon percentages for the MC3 stalagmite show similar systematic variations, in that values are higher during the late glacial, Older Dryas, Inter-Allerød Cold period, and the onset of the YD, intervals when the $\delta^{13}C$ record suggests wetter conditions above the cave and lowest during inferred drier periods characterized by more positive $\delta^{13}C$ (Fig. 4). Both the carbonate host-rock and accumulated soil organic matter (SOM) overlying a cave can contribute carbon that is depleted in ^{14}C ('dead carbon') to drip waters, in particular if SOM above the cave has a long (millennial-scale) turnover rate (Genty et al., 2001). Thus, peaks in dcp in the Moaning Cave record could reflect periods of increased host-rock dissolution, increased contribution of carbon from old SOM, or a combination of both sources.

Stalagmite MC3 $^{87}Sr/^{86}Sr$ ratios reflect varying contributions from two end-members: a less radiogenic soil source with an average value of 0.70489 ± 0.0011 derived from the weathering of metamorphic and altered volcanic rocks above Moaning Cave and a more radiogenic host-carbonate source with an average value of 0.70744 ± 0.00036 (Oster et al., 2009). Other potential sources of Sr to the Moaning Cave seepage water, and thus the stalagmite, include seaspray and wind-borne dust. Seawater $^{87}Sr/^{86}Sr$ presently ranges from 0.70916 to 0.70923 (DePaolo and Ingram, 1985; Palmer and Edmond, 1989) and has not fallen below 0.70915 during the Pleistocene (Capo and DePaolo, 1990). As the Moaning Cave stalagmite $^{87}Sr/^{86}Sr$ ratios are never more radiogenic than the host marble values, it is unlikely that seaspray provided a significant source of Sr to cave seepage water. The largest potential dust source to Moaning Cave is California's Central Valley, which is located to the west of the Sierra Nevada (Fig. 1B). The Central Valley is dominated by the Sacramento and San Joaquin River systems, with the Sacramento River and its tributaries draining the northern Sierra Nevada and the San Joaquin and its tributaries draining the southern Sierra Nevada. Suspended load sediments in the Sacramento River have $^{87}Sr/^{86}Sr$ ratios that range from 0.7039 to 0.7056, while San Joaquin sediments range from 0.7063 to 0.7083. $^{87}Sr/^{86}Sr$ ratios of sediment cores from the San Francisco Bay estuary, where both rivers empty into the Pacific Ocean, suggest that the relative influx of sediment from these two river systems has varied over the past ~2000 years, and it is hypothesized that this variability is related to the position of storm tracks over California (Ingram and Lin, 2002). If this hypothesis is correct, during Northern Hemisphere warm periods, when the storm tracks are situated further north, the San Francisco Bay estuary should be dominated by sediments from the Sacramento River drainage, which have relatively less radiogenic $^{87}Sr/^{86}Sr$ values. This hypothesis, however, would require regional climate modeling to test further. As $^{87}Sr/^{86}Sr$ ratios in the Moaning Cave stalagmite are generally more radiogenic during Northern Hemisphere warm periods, it is unlikely that

Table 2
^{14}C data and dead carbon proportion for Moaning Cave stalagmite samples.

CAMS #	Depth (mm)	U/Th age model (cal BP)	Frac. modern (measured)	$a^{14}C_{init}$ (pM)	$a^{14}C_{atm}$ (pM)	calibrated ^{14}C age (cal year BP)	dcp (%)
126151	12.0	8810	0.3331 ± 0.0013	96.71	107.4	9845 ± 114	9.96
141720	14.0	8837	0.3277 ± 0.0010	95.44	108.1	10172 ± 52	11.71
139888	16.0	8863	0.3262 ± 0.0011	95.31	108.3	10196 ± 40	11.97
141723	16.8	8873	0.3322 ± 0.0012	97.17	108.2	10069 ± 86	10.17
141719	17.0	8877	0.3306 ± 0.0012	96.75	108.2	10039 ± 130	10.56
141722	18.2	8977	0.3200 ± 0.0010	94.79	109.7	10271 ± 34	13.59
126154	20.0	9757	0.3123 ± 0.0013	101.68	109.1	10586 ± 93	6.82
141721	20.9	10169	0.2951 ± 0.0010	100.98	112.5	11222 ± 28	10.25
139885	21.0	10200	0.2967 ± 0.0010	101.90	111.9	11202 ± 35	8.91
141716	21.9	10558	0.2622 ± 0.0010	94.05	112.3	12670 ± 68	16.25
126149	22.7	11401	0.2868 ± 0.0010	113.90	114.3	12797 ± 58	0.36
141717	23.0	12140	0.2528 ± 0.0011	109.77	119.7	12937 ± 138	8.30
139886	24.4	12230	0.2475 ± 0.0010	108.69	120.7	13125 ± 88	9.95
139887	25.6	12356	0.2387 ± 0.0010	106.42	122.2	13338 ± 76	12.91
141718	26.0	12429	0.2443 ± 0.0012	109.87	121.0	13197 ± 83	9.23
126153	26.1	12443	0.2434 ± 0.0010	109.66	121.5	13215 ± 77	9.77
139884	27.5	12676	0.2464 ± 0.0010	114.19	124.0	13157 ± 74	7.88
141715	31.5	13343	0.2168 ± 0.0009	108.88	119.8	14156 ± 157	9.12
141714	34.5	13839	0.2161 ± 0.0009	115.29	119.7	14213 ± 187	3.65
139883	36.3	14139	0.2052 ± 0.0009	113.52	119.9	15072 ± 241	5.30
139882	37.5	14338	0.2054 ± 0.0009	116.37	120.8	15050 ± 241	3.67
139881	40.5	14837	0.1960 ± 0.0009	117.93	126.1	15870 ± 434	6.45
139880	43.0	15042	0.1914 ± 0.0009	118.11	126.3	16197 ± 354	6.52
139879	46.0	15226	0.1958 ± 0.0009	123.49	126.3	15881 ± 432	2.22
139878	49.0	15409	0.1892 ± 0.0010	122.05	126.9	16397 ± 296	3.82
139889	54.5	15746	0.1871 ± 0.0009	125.71	128.5	16566 ± 194	2.17
126156	62.0	16204	0.1745 ± 0.0008	123.93	130.3	17085 ± 120	4.86
126150	67.0	16510	0.1696 ± 0.0008	124.95	131.2	17333 ± 179	4.76

variations in the input of dust from the Central Valley control stalagmite ^{87}Sr/^{86}Sr values. Rather, the most conservative and likely explanation for the observed stalagmite ^{87}Sr/^{86}Sr values is variation in the contribution of Sr to cave seepage waters from soil and host-rock sources directly above Moaning Cave.

Thus, stalagmite MC3 ^{87}Sr/^{86}Sr ratios provide a proxy of groundwater–host-rock interaction in the epikarst that is independent of dcp. Less radiogenic speleothem ^{87}Sr/^{86}Sr ratios during inferred periods of increased precipitation (late glacial, Older Dryas, Inter-Allerød Cold period, and the onset of the YD), are interpreted to record an increased contribution of soil-derived Sr due to rapidly infiltrating precipitation and short residence times of seepage waters in the host carbonate, following the approach of Banner et al. (1996). The more radiogenic speleothem ^{87}Sr/^{86}Sr ratios during inferred drier periods, record increased seepage-water residence time in the carbonate aquifer and increased meteoric water–marble interaction.

Through the entire record, MC3 dcp values are only weakly correlated with ^{87}Sr/^{86}Sr ($r^2 = 0.30$), although the resolution of the dcp record is much lower than that of the ^{87}Sr/^{86}Sr record (Fig. 4). The overall lack of a correlation between the two records and shifts to less radiogenic ^{87}Sr/^{86}Sr during periods of increased dcp, however, suggests that variation in host-carbonate dissolution was likely not the primary influence on observed changes in dcp. Rather, this relationship suggests that the recalcitrant fraction of

SOM may have been a major contributor of dead carbon to seepage water and thus to stalagmite calcite δ^{13}C values.

The age of SOM directly above Moaning Cave has not been determined, however, studies of modern soil carbon cycling at other Sierra Nevada sites at both higher and lower elevations than Moaning Cave, indicate relatively short residence times for soil carbon. For example, SOM at a forested site at 1300 m elevation on the western slope of the Sierra Nevada is made up of approximately equal fractions of carbon with 10-, 100-, and 1000-year residence times (Trumbore, 1993). This SOM would have a mean residence time of 370 years, which would be equivalent to a dead carbon content of ∼3%, assuming a half-life for ^{14}C of 5730 years. This suggests that the contribution of SOM to dead carbon in the Moaning Cave system at present is similar to that in warm intervals of the early B-A and during the middle YD. For all other times of the Moaning Cave record, dcp is higher, suggesting a higher contribution of SOM than present day. If all of the dead carbon in the Moaning Cave stalagmite originated from aging SOM, then the range of dcp variability noted in the MC3 record (from an initial deglacial value of 11% at 16.5 ka, to the maximum value of 16% at 10.6 ka) would represent about a 600 year increase in the mean age of SOM above the cave during much of the last deglacial.

Periods of elevated dead carbon in the Moaning Cave stalagmite (16.5–15.8, 13.3–12.1, 10.5–10.2, 8.8–8.5 ka, Fig 4B) coincide with intervals of the most negative
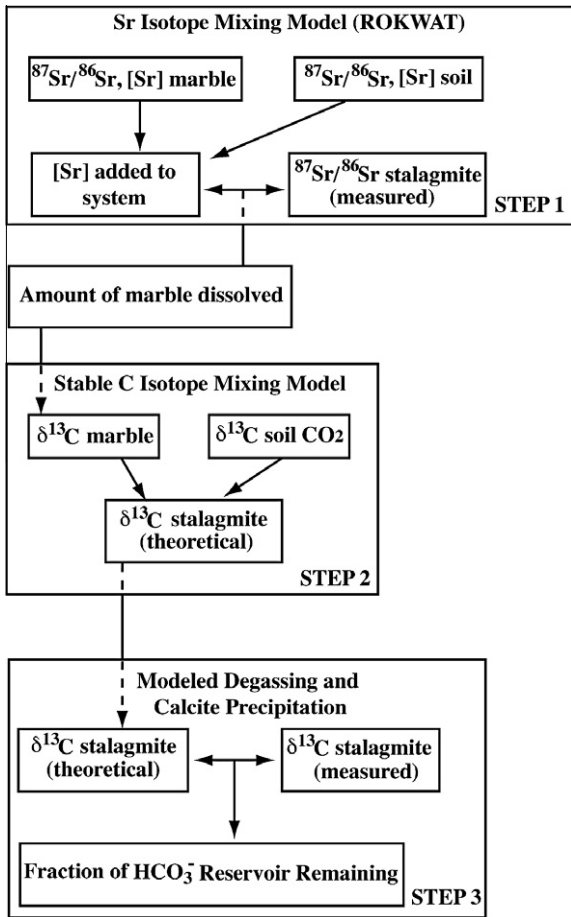
Sr Isotope Mixing Model (ROKWAT)

$^{87}Sr/^{86}Sr$, [Sr] marble

$^{87}Sr/^{86}Sr$, [Sr] soil

[Sr] added to system

$^{87}Sr/^{86}Sr$ stalagmite (measured)

STEP 1

Amount of marble dissolved

Stable C Isotope Mixing Model

$\delta^{13}C$ marble

$\delta^{13}C$ soil CO_2

$\delta^{13}C$ stalagmite (theoretical)

STEP 2

Modeled Degassing and Calcite Precipitation

$\delta^{13}C$ stalagmite (theoretical)

$\delta^{13}C$ stalagmite (measured)

Fraction of HCO_3^- Reservoir Remaining

STEP 3

Fig. 5. Schematic of mixing models and degassing calculations used for this study (see text for description of models).

measured $\delta^{13}C$ values. During these intervals, Greenland ice core records indicate decreased temperatures at high northern latitudes (Stuiver and Grootes, 2000; Andersen et al., 2005; Svensson et al., 2006) and additional Moaning Cave stalagmite proxy records ($\delta^{18}O$, trace element contents) suggest that the climate above the cave was wetter and possibly colder (Oster et al., 2009). Elevated dcp during these cold, wet intervals could be explained by increased accumulation relative to oxidative decay of organic matter, leading to longer mean residence times for SOM above Moaning Cave. Periods of lower dcp and less negative $\delta^{13}C$ values, therefore, indicate higher SOM turnover rates during warm, dry periods of the past deglacial. These results are consistent with studies of modern soils that document increased rates of SOM decomposition in warmer and drier climates (e.g., Raich and Schlesinger, 1992; Davidson and Janssens, 2006).

5.2. Constraining host-carbonate dissolution using stalagmite $^{87}Sr/^{86}Sr$ ratios

As dcp in the Moaning Cave stalagmite is not primarily controlled by changes in host-carbonate dissolution, it is not an accurate proxy of the influence of water–rock interaction on speleothem $\delta^{13}C$. We use speleothem $^{87}Sr/^{86}Sr$ as

a proxy of the degree of groundwater interaction with the host marble in order to constrain, independently of dcp, the contribution of variation in host-rock dissolution to the Moaning Cave $\delta^{13}C$ record. The geochemical model, ROKWAT (Banner and Hanson, 1990; Banner et al., 1989) was used to simulate the interaction of soil waters with the Moaning Cave host marble. The model defines an initial solution of [Sr], [Ca], and $^{87}Sr/^{86}Sr$ that interacts with a host carbonate of specified [Sr], $^{87}Sr/^{86}Sr$, and porosity. For the Moaning Cave system, the starting solution is the average of the weakest (ammonium acetate) soil leachates ([Sr] = 0.029 ppm, [Ca] = 5.1 ppm, $^{87}Sr/^{86}Sr$ = 0.705354) and the host carbonate is the Moaning Cave marble ([Sr] = 298 ppm, $^{87}Sr/^{86}Sr$ = 0.707435). [Sr] and $^{87}Sr/^{86}Sr$ of the resulting fluid is calculated as the water and rock interact (Fig. 6). The amount of strontium that must have been derived from the host marble in order to form stalagmite calcite with the observed $^{87}Sr/^{86}Sr$ ratios can be constrained given that there is negligible Sr isotope fractionation between calcite and the fluid from which it precipitates (Banner and Kaufman, 1994). In turn, from these values and the average Sr concentration of the host marble, an approximate amount of dissolved marble necessary to reach each measured speleothem $^{87}Sr/^{86}Sr$ value is inferred (Fig. 6).

5.3. Modeling stalagmite $\delta^{13}C$ derived from host-carbonate and soil CO_2

The strontium isotopic mixing model constrains the amount of host marble contribution of Sr to the MC3 speleothem during precipitation, and thus can be used to estimate the influence of variation in host-rock dissolution on the Moaning Cave carbon isotope record during the last deglacial. To investigate this, we constructed a two-component mixing model of the carbon isotope system for Moaning Cave (described below) from which a theoretical $\delta^{13}C$ value of stalagmite calcite that precipitated in isotopic
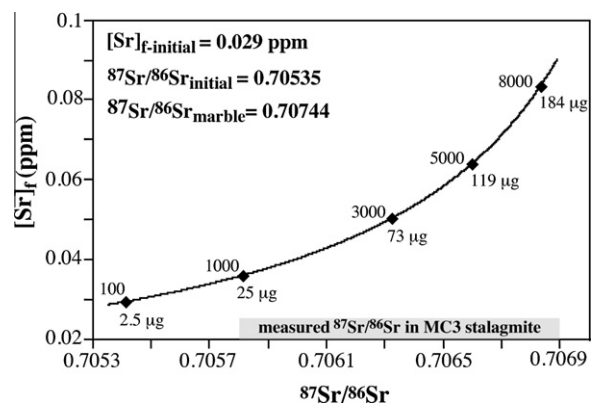

Fig. 6. Concentration of Sr in the fluid versus fluid $^{87}Sr/^{86}Sr$ for model of fluid interaction with carbonate host using ROKWAT. Starting composition of fluid is shown. Diamonds indicate number of model iterations (top) (the equivalent of pore volumes of fluid) and amount of marble dissolved (bottom) for increments of the model. Gray box outlines the range of measured $^{87}Sr/^{86}Sr$ for the MC3 stalagmite.

equilibrium with the fluid is calculated (Table 3). The residual difference between the theoretical and measured stalagmite $\delta^{13}C$ records is inferred to result from CO_2 degassing and calcite precipitation upflow from the speleothem drip site.

Table 3
MC3 $^{87}Sr/^{86}Sr$, $\delta^{13}C_{DIC}$ in equilibrium with measured speleothem $\delta^{13}C$, modeled $\delta^{13}C_{HCO_{3-f}}$, and fraction of $HCO_3^-{}_{(aq)}$ remaining in solution for the 20% and 40% maximum hrc.

Depth (mm)	U-series age (kyr)	$^{87}Sr/^{86}Sr$ (meas.)	$^{13}C_{DIC}$ meas.	Sr added (ppm)	$\delta^{13}C_{HCO_{3-f}}$ (modeled) 20% max	$\delta^{13}C_{HCO_{3-f}}$ (modeled) 40% max	$f\ HCO_3^-$ remaining 20% max	$f\ HCO_3^-$ remaining 40% max
9	8.77	0.706329	−8.47	0.0219	−14.81	−13.63	0.20	0.27
12	8.81	0.706300	−9.29	0.0208	−14.87	−13.75	0.24	0.32
15.5	8.86	0.706266	−8.98	0.0195	−14.94	−13.89	0.22	0.28
17	8.88	0.706254	−9.16	0.0191	−14.96	−13.93	0.23	0.29
20	9.76	0.706255	−11.86	0.0191	−14.96	−13.93	0.45	0.59
20.3	9.89	0.706105	−11.94	0.0143	−15.22	−14.44	0.43	0.53
20.5	9.97	0.706267	−11.65	0.0195	−14.94	−13.89	0.43	0.56
20.95	10.17	0.706223	−11.96	0.0180	−15.02	−14.05	0.46	0.58
21	10.19	0.706162	−11.95	0.0160	−15.12	−14.26	0.44	0.55
	10.20	0.706456	−12.05	0.0274	−14.51	−13.03	0.53	0.78
21.2	10.28	0.706177	−11.95	0.0165	−15.10	−14.21	0.45	0.56
	10.56	0.706493	−11.38	0.0293	−14.41	−12.83	0.46	0.69
23	12.14	0.706301	−10.94	0.0208	−14.87	−13.75	0.36	0.49
23.5	12.17	0.706291	−11.55	0.0204	−14.89	−13.79	0.42	0.56
25	12.26	0.706263	−11.93	0.0194	−14.95	−13.90	0.46	0.60
	12.36	0.706364	−11.67	0.0233	−14.73	−13.48	0.46	0.63
27	12.59	0.706261	−8.98	0.0193	−14.95	−13.91	0.22	0.28
28	12.76	0.706014	−8.61	0.0119	−15.35	−14.71	0.18	0.21
29	12.93	0.706890	−9.22	0.0615	−12.68	−9.37	0.41	0.96
30.5	13.17	0.706447	−9.49	0.0270	−14.53	−13.08	0.27	0.40
31	13.26	0.706138	−9.76	0.0153	−15.16	−14.34	0.25	0.31
32.5	13.51	0.706136	−8.44	0.0152	−15.17	−14.35	0.18	0.22
32.76	13.55	0.706187	−8.90	0.0168	−15.08	−14.18	0.20	0.26
33	13.59	0.706129	−9.37	0.0150	−15.18	−14.37	0.23	0.28
34	13.76	0.705964	−8.03	0.0106	−15.42	−14.84	0.15	0.17
35	13.92	0.706028	−8.06	0.0122	−15.33	−14.67	0.16	0.18
36	14.09	0.706355	−9.94	0.0229	−14.75	−13.52	0.29	0.40
37	14.26	0.706284	−7.89	0.0202	−14.90	−13.82	0.17	0.22
38	14.42	0.706419	−7.48	0.0257	−14.60	−13.22	0.16	0.23
39	14.59	0.706646	−7.29	0.0386	−13.91	−11.83	0.18	0.31
40	14.75	0.706220	−7.17	0.0179	−15.03	−14.06	0.13	0.17
40.5	14.84	0.706396	−7.79	0.0247	−14.66	−13.33	0.17	0.24
41	14.92	0.706018	−7.00	0.0120	−15.34	−14.70	0.12	0.14
42	14.98	0.706068	−8.72	0.0133	−15.27	−14.56	0.19	0.22
43	15.04	0.705964	−10.72	0.0106	−15.42	−14.84	0.30	0.35
43.5	15.07	0.705772	−7.71	0.0065	−15.64	−15.29	0.13	0.14
44.25	15.12	0.706151	−9.49	0.0119	−15.35	−14.71	0.22	0.26
45	15.16	0.706068	−9.49	0.0133	−15.27	−14.55	0.23	0.27
46	15.23	0.705965	−9.49	0.0107	−15.42	−14.84	0.22	0.25
47	15.29	0.706122	−10.26	0.0148	−15.19	−14.39	0.28	0.35
48	15.35	0.706164	−10.12	0.0161	−15.12	−14.26	0.28	0.35
49	15.41	0.706171	−10.05	0.0163	−15.11	−14.23	0.27	0.34
50	15.47	0.706073	−9.95	0.0134	−15.27	−14.54	0.26	0.31
51	15.53	0.705818	−10.28	0.0074	−15.59	−15.19	0.26	0.28
52	15.59	0.705970	−10.23	0.0108	−15.41	−14.83	0.26	0.31
53	15.65	0.706036	−10.31	0.0124	−15.32	−14.65	0.28	0.33
54.5	15.75	0.705915	−10.17	0.0095	−15.48	−14.97	0.26	0.29
56	15.84	0.705905	−9.77	0.0093	−15.49	−14.99	0.23	0.26
57	15.90	0.706029	−10.21	0.0123	−15.33	−14.67	0.27	0.32
58	15.96	0.706237	−10.24	0.0185	−14.99	−14.00	0.30	0.38
59	16.02	0.706241	−9.65	0.0186	−14.99	−13.98	0.25	0.33
60	16.08	0.706143	−9.65	0.0154	−15.16	−14.33	0.24	0.30
61	16.14	0.705957	−9.93	0.0105	−15.43	−14.86	0.24	0.28
62	16.20	0.706204	−9.93	0.0174	−15.05	−14.12	0.27	0.34
63	16.27	0.705994	−9.66	0.0114	−15.38	−14.76	0.23	0.27
64	16.33	0.706265	−9.66	0.0195	−14.94	−13.89	0.26	0.34

The amount of marble that dissolved at each step (i.e., the output from the Sr-based model; Fig. 5 and Table 3) was converted to a percentage of host-rock carbon contribution to total seepage-water DIC. These values were then scaled to reflect potential upper and lower limits of host-rock contribution of carbon to DIC that have been previously determined based on models and observations of modern cave systems. In a model of a fully closed-system cave environment, Hendy (1971), found that up to 50% of carbon in solution can be host-rock derived. Caves are generally not fully closed-system environments (McDermott, 2004), however, and field observations of European cave systems suggest soil CO_2 contributes between 80% and 95% of speleothem carbon (Genty and Massault, 1999; Genty et al., 1999, 2001). As Moaning Cave, a fracture dominated cave system, is unlikely to be a fully closed-system, we modeled two scenarios, one in which the host-rock contributes 0–20% of the carbon in DIC, and another in which it contributes 0–40%.

We calculated δ^{13}C values of stalagmite calcite that would have precipitated in equilibrium with seepage water of theoretical δ^{13}C values of DIC. Theoretical DIC δ^{13}C was calculated using two end-member sources (1) host-rock carbon (δ^{13}C = 0.6‰) contribution constrained by the Sr-based mixing model, and (2) soil CO_2 associated with Moaning Cave (Table 3). Plants that utilize the C_3 photosynthetic pathway are the dominant vegetation in the Sierra Nevada foothills, and there is no pollen or packrat midden evidence for C_4 flora in the greater study region over the past 20+ ky (Davis, 1999; Thompson et al., 1993; Cole, 1983). Accordingly, to estimate soil CO_2 δ^{13}C we used the δ^{13}C of modern leaf litter and root material collected above Moaning Cave (−25.4‰ to −32.8‰, $n = 12$) to represent the δ^{13}C of soil organic material throughout the interval from 16.4 to 8.8 ka. Soil CO_2 derived from decay of this material and root respiration should range between −21‰ and −28.4‰, taking into account the 4.4‰ fractionation caused by the differing diffusion coefficients for $^{12}CO_2$ and $^{13}CO_2$ (Cerling et al., 1991). Equilibrium fractionation between soil $CO_{2(g)}$ and $HCO_3^-{}_{(aq)}$ at 16.2 °C (Table 4) would result in δ^{13}C$_{DIC}$ values between −19.7‰ and −12.3‰ for the soil-derived end-member. We used this temperature, which is the measured average winter temperature at the Moaning Cave stalagmite collection site (2005–2007), as drip sites are currently only active and the majority of calcite precipitation occurs during winter months in Moaning Cave. Thus, this provides a minimum fractionation value. How past soil temperatures above the cave varied is unknown, however the temperature would most likely

have been lower during the deglacial and YD. For comparison, the δ^{18}O of planktonic foraminifera in the Santa Barbara Basin suggest that sea surface temperatures decreased by ~4 °C at the onset of the YD (Hendy et al., 2002). A similar reduction in winter temperatures at Moaning Cave would result in soil end-member δ^{13}C$_{DIC}$ values shifted to −19.2‰ and −11.8 ‰ (Table 4), yielding modeled stalagmite δ^{13}C values that are elevated by only ⩽0.4‰ relative to the warmer temperature used in our model.

A value for the δ^{13}C$_{DIC}$ (δ^{13}C$_{HCO_{3-f}}$) was determined using the equation:

$$\delta^{13}\text{C}_{\text{HCO}_{3-f}} = (F_{\text{C-Sr}} * \delta^{13}\text{C}_{\text{marb}}) + ((1 - F_{\text{C-Sr}}) * \delta^{13}\text{C}_{\text{soil}}),$$

(3)

where $F_{\text{C–Sr}}$ is the fraction of carbon contributed from the host carbonate derived from the Sr-based mixing model. We computed δ^{13}C$_{HCO_{3-f}}$ using host-rock contributions (hrc) based on both the 20% and 40% maximum contribution limits (Table 3). Modeled δ^{13}C values for HCO$_{3-f}$ fall between −12.7‰ and −15.6‰ for a 20% hrc and −9.4‰ and −15.3‰ for a 40% hrc. These values for δ^{13}C$_{DIC}$ fall within the range of values expected for seepage-water DIC in open (−14‰ to −18‰) and closed (−11‰) cave systems overlain by C_3 ecosystems and saturated with respect to CaCO$_3$ (Hendy, 1971; Dulinski and Rozanski, 1990), but are generally lower than measured winter δ^{13}C$_{DIC}$ for Moaning Cave drip water (−10.2‰ to −8.4‰, $n = 2$). Average ^{87}Sr/^{86}Sr measurement error (4.5×10^{-5}) when propagated through the Sr and the carbon mixing models results in errors of ±0.1‰ on the 20% hrc values and ±0.2‰ on the 40% hrc values.

The dampened degree of variability in the modeled δ^{13}C relative to that delineated by measured stalagmite δ^{13}C (Fig. 7) indicates that temporal changes in the degree of host-carbonate dissolution cannot account for the observed trends in measured δ^{13}C and dcp. Rather, the modeled δ^{13}C values suggest that variations in the contribution of carbon from SOM exerted the larger influence on speleothem δ^{13}C variability (and dcp) at Moaning Cave during the deglacial. More negative stalagmite δ^{13}C values during periods of wetter climate suggest increased ecosystem productivity, which coupled with possibly less well-drained soils, would have favored organic matter accumulation, an increased proportion of refractory organic carbon, and longer mean ages of the SOM reservoir. In contrast, the less negative δ^{13}C values associated with warm, dry periods, suggest overall lower soil productivity that would have led to more rapid SOM turnover rates in better drained soils.

Comparison of measured stalagmite δ^{13}C (Fig. 7A) with model predictions of δ^{13}C$_{carb}$ (Fig. 7B) also indicates that, with the exception of one point at 12.9 ka, values for stalagmite δ^{13}C cannot be successfully predicted using the two-component mixing model alone. Accordingly, we conclude that an additional process must have influenced stalagmite δ^{13}C. Two such additional processes that could influence stalagmite δ^{13}C are: (1) kinetic effects during calcite precipitation and (2) ^{13}C-enrichment of the $HCO_3^-{}_{(aq)}$ reservoir due to CO_2 degassing and calcite precipitation upflow from the speleothem drip site (Baker et al., 1997; Fairchild et al., 2000; Mickler et al., 2004).

Table 4
Carbon isotope fractionation factors (1000 ln α).

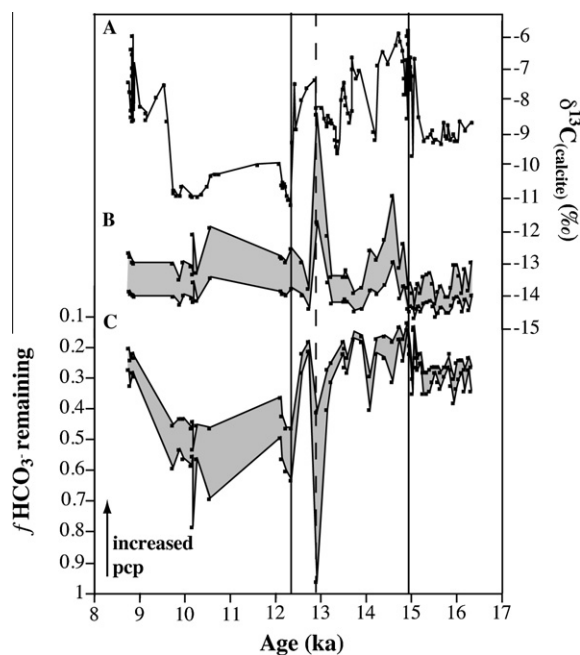| Species pair	Fractionation factor (‰) 16.2 °C	Fractionation factor (‰) 12.2 °C	Reference
CaCO$_3$–HCO$_3^-{}_{(aq)}$	1.0	1.0	Romanek et al. (1992)
HCO$_3^-{}_{(aq)}$–CO$_{2(g)}$	8.9	9.4	Zhang et al. (1995)

Fig. 7. (A) Measured MC3 $\delta^{13}C$ and (B) modeled speleothem $\delta^{13}C$ for 20% (bottom curve), 40% (top curve) maximum host-rock contribution (hrc). (C) Fraction of HCO_3^- remaining in solution after degassing and prior calcite precipitation is shown for 20% (upper curve) and 40% (lower curve) maximum hrc. Black lines tie the onset of the B-A ($\sim$14.9 ka) and YD ($\sim$12.4) in the MC3 $\delta^{13}C$ record. Dashed line highlights a spike in host-carbonate dissolution defined by an increase to maximum stalagmite $^{87}Sr/^{86}Sr$ ratios leading to modeled speleothem $\delta^{13}C$ values that closely approximate the measured value. Given that this spike is defined by one speleothem $^{87}Sr/^{86}Sr$ ratio, it cannot be confidently interpreted to have climatic significance.

Moaning Cave stalagmite $\delta^{18}O$ and $\delta^{13}C$ values exhibit significant down axis correlation ($r^2 = 0.81$) that could be interpreted to record non-equilibrium isotope precipitation (e.g., Hendy, 1971; Mickler et al., 2006). In order to empirically test for the influence of kinetic effects in stalagmite MC3, we analyzed partial $\delta^{18}O$ and $\delta^{13}C$ profiles in three off-axis cores (MC3-B, MC3-C, and MC3-D). We chose to analyze off-axis $\delta^{18}O$ and $\delta^{13}C$ profiles given the documented shortcomings of, and difficulty in, performing traditional Hendy tests for kinetic processes (e.g., Mickler et al., 2006; Dorale and Liu, 2009). All four cores display similar $\delta^{18}O$ and $\delta^{13}C$ values, and excursions are reproduced in two off-axis cores (Oster et al., 2009). The ability to reproduce $\delta^{18}O$ and $\delta^{13}C$ in off-axis cores suggests that kinetic effects did not significantly influence the stable isotope values in the MC3 stalagmite and cannot account for the difference between modeled and measured stalagmite $\delta^{13}C$ values delineated in this study. The differences in modeled and measured $\delta^{13}C$ values thus likely record the influence of degassing and attendant prior calcite precipitation upflow from the speleothem drip site. Such processes are particularly common in semi-arid, highly seasonal epikarst environments, leading to more ^{13}C-enriched drip water and speleothem calcite (e.g., Baker et al., 1997).

5.4. Effects of degassing and calcite precipitation in the epikarst

The calcite dissolution/precipitation equation can be written as follows:

$$2HCO_3^- + Ca^{2+} \Longleftrightarrow CaCO_3 + H_2O + CO_2 \qquad (4)$$
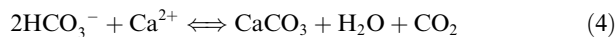
Equilibrium fractionation factors between $CO_{2(g)}$ and HCO_3^- and $CaCO_3$ and HCO_3^- at the average winter temperature in Moaning Cave (16.2 °C) are given in Table 4. The $\delta^{13}C$ value of the $HCO_{3\ (aq)}^-$ reservoir follows Rayleigh-type enrichment in ^{13}C with progressive degassing, as the loss of isotopically light ^{12}C from degassing cannot be offset by the loss of isotopically heavier ^{13}C through calcite precipitation (Mickler et al., 2004), assuming a one for one loss of CO_2 and $CaCO_3$. The effects of this Rayleigh distillation due to degassing and calcite precipitation on measured Moaning Cave stalagmite $\delta^{13}C$ values can be modeled using the equation:

$$(\delta^{13}C_{HCO_3^-} + 1000)/(\delta^{13}C_{HCO_{3\ f}^-} + 1000) = f(\alpha_{p-r}^{-1}); \qquad (5)$$

where $\delta^{13}C_{HCO_3^-}$ is the isotopic composition of $HCO_{3\ (aq)}^-$ in equilibrium with measured speleothem $\delta^{13}C$, $\delta^{13}C_{HCO_{3-f}}$ is the isotopic composition of $HCO_{3\ (aq)}^-$ before degassing (Eq. (3)), and f is the fraction of $HCO_{3\ (aq)}^-$ remaining in solution following degassing (Mickler et al., 2004; Bar-Matthews et al., 1996). The fractionation factor (α_{p-r}) between $HCO_{3\ (aq)}^-$ and the bulk product of $CO_{2(g)}$ and precipitated $CaCO_3$ is defined following Mickler et al. (2004) as:

$$\alpha_{p-r} = \frac{1}{2}(\alpha_{CO_2-HCO_3^-}) + \frac{1}{2}(\alpha_{CaCO_3-HCO_3^-}) \qquad (6)$$

given that the C in $HCO_{3\ (aq)}^-$ is evenly divided between $CO_{2(g)}$ and $CaCO_3$ solid during degassing and precipitation.

The results of the degassing calculations for the MC3 record demonstrate that a substantial amount of the observed variability in Moaning Cave $\delta^{13}C$ is due to changes in the degree of degassing and prior calcite precipitation between warm, dry, and cold, wet periods of the past deglacial. Estimated lower fractions of $HCO_{3\ (aq)}^-$ remaining in solution, and thus higher degrees of prior calcite precipitation, correlate with more positive speleothem $\delta^{13}C$, whereas, higher fractions of $HCO_{3\ (aq)}^-$ remaining in solution and decreased amounts of prior calcite precipitation are associated with more negative $\delta^{13}C$ ($r = -0.85$ for 20% hrc and -0.54% for 40% hrc; Fig. 7). This relationship is consistent with the previously suggested hypothesis using coupled isotopic and trace element proxy records for the MC3 stalagmite (Oster et al., 2009), that northern hemisphere warm periods were associated with decreased rainfall above the cave, leading to decreased soil respiration (and higher stalagmite $\delta^{13}C$) and increased seepage-water residence time (and increased prior calcite precipitation) in the epikarst.

The overall fraction of $HCO_{3\ (aq)}^-$ remaining in solution (Fig. 7C), over the 20% maximum hrc (0.1–0.3) and 40% maximum hrc (0.1–0.4) range, however, is low during the late glacial and B-A relative to the period following the onset of the YD at $\sim$12.4 ka. The shift to overall higher values for the estimated fraction of $HCO_{3\ (aq)}^-$ remaining in solution is interpreted to record a substantial decrease in

degassing and prior calcite precipitation during the YD. This indicates that either seepage-water residence times were significantly decreased or cave air pCO_2 was higher due to decreased seasonal cave ventilation during the YD as compared to the early deglacial and B-A (Banner et al., 2007; James and Banner, 2008). If winters were colder during the YD, as is suggested by other regional proxy records (e.g., Vacco et al., 2005) and possibly also the Moaning Cave $\delta^{18}O$ record, mean surface air temperature and thus cave air temperature would have decreased. However, colder winters likely would have also led to enhanced difference between winter and summer surface air temperatures during the YD relative to the B-A. Thus, cave air ventilation was likely increased during the YD, leading to lower cave air pCO_2 relative to the B-A. As the estimated fraction of $HCO_3^-{}_{(aq)}$ remaining in solution is at its overall lowest (and therefore the amount of degassing is at its *highest*) during the B-A, it is unlikely that changes in cave ventilation can fully explain variations in prior calcite in the MC record. Rather, the estimated high fraction of $HCO_3^-{}_{(aq)}$ remaining in solution for the ~2000 year period between the onset of the YD continuing to ~9.7 ka, suggests that the YD in the central foothills of the Sierra Nevada was not only the wettest period of the past deglacial but that wet conditions persisted above Moaning Cave for an interval of time substantially longer than the conventionally defined YD (~12.9–11.5 ka) (Stuiver and Grootes, 2000; Andersen et al., 2005; Svensson et al., 2006).

Notably, the estimated fraction of $HCO_3^-{}_{(aq)}$ remaining in solution rarely rises above 0.7 even within inferred wet intervals characterized by highest seepage-water flow rates and soil respiration rates. This suggests that degassing and prior calcite precipitation in the Moaning Cave epikarst exerted an influence on stalagmite $\delta^{13}C$ values throughout its formation. While speleothem records have been developed from other similarly arid and semi-arid regions, such as the Levant region (e.g., Ayalon et al., 1999; Frumkin et al., 2000; Verheyden et al., 2008), Oman and Yemen (e.g., Neff et al., 2001; Fleitmann et al., 2007; Shakun et al., 2007), and the western United States (e.g., Polyak et al., 2004; Asmerom et al., 2007, 2010; Denniston et al., 2007; Wagner et al., 2010), such cave systems are less well studied relative to those from humid and sub-humid environments (e.g., China, Europe, the Midwestern United States). Notably, a study of stalactite drip waters from the semi-arid Soreq Cave system, Israel, documented that up to 85% of the drip water HCO_3^- reservoir can be lost due to degassing and prior calcite precipitation (Bar-Matthews et al., 1996). Furthermore, Mickler et al. (2006) found that degassing and prior calcite precipitation may have significantly influenced up to 55% of published speleothem stable isotope records ($n = 128$). This study further documents the importance of assessing the effects of degassing and prior calcite precipitation in the interpretation of speleothem $\delta^{13}C$ records, in particular for those from caves in semi-arid to arid environments, and provides a quantitative approach to constraining these processes in paleo-cave environments. In turn, an ability to better constrain the various soil and epikarst processes that govern speleothem $\delta^{13}C$ values greatly expands the potential of stable isotope records for reconstructing past climate changes above cave systems. The integrated use of ^{14}C, $^{87}Sr/^{86}Sr$, and geochemical modeling may provide the necessary framework for interpreting complex speleothem $\delta^{13}C$ records, which are published much less frequently than records of speleothem $\delta^{18}O$ variability, but have the potential to provide valuable insight into regional changes in effective moisture.

6. CONCLUSIONS

A record of dead carbon proportion (dcp), estimated from coupled stalagmite calcite ^{14}C and $^{230}Th/U$ measurements and independently calibrated records of atmospheric radiocarbon content, was developed for a Moaning Cave stalagmite (MC3). The dcp for this stalagmite is not well correlated with $^{87}Sr/^{86}Sr$, an independent proxy of water–rock interaction, suggesting that variations in dcp do not solely reflect changes in host-rock dissolution. Increases in dcp during intervals of decreased stalagmite $\delta^{13}C$ indicate a varying yet substantial contribution from the soil OM reservoir, likely due to significantly increased average residence time of SOM in the soil veneer above the cave during wet periods. These results may have implications for speleothem ^{14}C records that use constant dcp corrections through time or that assume all speleothem dead carbon is derived from the carbonate host-rock (e.g., Hoffmann et al., 2010; Beck et al., 2001).

A three-step approach allows us to evaluate the contribution of soil organic carbon and host-rock dissolution to seepage-water DIC and to assess the degree to which degassing and prior calcite precipitation in the epikarst influenced the measured stalagmite $\delta^{13}C$ values at Moaning Cave during the past deglacial. The Moaning Cave dcp, degassing calculations, and $\delta^{13}C$ and $^{87}Sr/^{86}Sr$ records suggest that Northern Hemisphere cold periods during the last deglaciation (late glacial, Older Dryas, Inter- Allerød Cold Period, YD) were associated with an increase in the average residence time of soil OM and elevated soil pCO_2, decreased water–rock interaction, and decreased degassing and prior calcite precipitation for the Moaning Cave system. This is consistent with wetter conditions in the central Sierra Nevada during these Northern Hemisphere cold periods.

Modeled $\delta^{13}C$ values and degassing calculations for the Moaning Cave stalagmite demonstrate that some degree of degassing and prior calcite precipitation in the epikarst occurred throughout the period recorded by the stalagmite. This documents the strong, yet variable, influence of these processes on the speleothem C isotope records, in particular from arid and semi-arid environments. The coupled radiogenic and stable isotope analysis integrated with the geochemical mixing model approach illustrated by this study provides a quantitative strategy to better constrain these processes in modern and paleo karst systems.

REFERENCES

Andersen K. K., Svensson A., Johnsen S. J., Rasmussen S. O., Bigler M., Röthlishberger R., Ruth U., Siggaard-Andersen M.-L., Steffensen J. P., Dahl-Jensen D., Vinther B. M. and Clausen H. B. (2005) The Greenland ice core chronology 2005, 15–42 ka. Part 1: Constructing the time scale. *Quaternary Sci. Rev.* **25**, 3246–3257.

Asmerom Y., Polyak V., Burns S. and Rassmussen J. (2007) Solar forcing of Holocene climate: new insights from a speleothem record, southwestern United States. *Geology* **35**, 1–4.

Asmerom Y., Polyak V. and Burns S. J. (2010) Variable moisture in the southwestern United States linked to rapid glacial climate shifts. *Nat. Geosci.* **3**, 114–117.

Ayalon A., Bari-Matthews M. and Kaufman A. (1999) Petrography, strontium, barium, and uranium concentrations, and strontium and uranium isotope ratios in speleothems as palaeoclimatic proxies: Soreq Cave, Israel. *Holocene* **9**. doi:10.1191/095968399673664163.

Baker A., Ito E., Smart P. L. and McEwan R. F. (1997) Elevated and variable values of ^{13}C in speleothems in a British cave system. *Chem. Geol.* **136**, 263–270.

Baker A., Genty D., Dreybrodt W., Barnes W., Mockler N. and Grapes J. (1998) Testing theoretically predicted stalagmite growth rate with recent annually laminated samples: implications for past stalagmite deposition. *Geochim. Cosmochim. Acta* **62**, 393–404.

Banner J. L., Wasserburg G. J., Dobson P. F., Carpenter A. B. and Moore C. H. (1989) Isotopic and trace element constraints on the origin and evolution of saline groundwaters from central Missouri. *Geochim. Cosmochim. Acta* **53**, 383–398.

Banner J. L. and Hanson G. N. (1990) Calculation of simultaneous isotopic and trace element variations during water–rock interaction with applications to carbonate diagenesis. *Geochim. Cosmochim. Acta* **54**, 3123–3137.

Banner J. L. and Kaufman J. (1994) The isotopic record of ocean chemistry and diagenesis preserved in non-luminescent brachiopods from Mississippian carbonate rocks, Illinois and Missouri. *Geol. Soc. Am. Bull.* **106**, 1074–1082.

Banner J. L., Musgrove M., Asmerom Y., Edwards R. L. and Hoff J. A. (1996) High-resolution temporal record of Holocene ground-water chemistry: tracing links between climate and hydrology. *Geology* **24**, 1049–1053.

Banner J. L., Guilfoyle A., James E. W., Stern L. A. and Musgrove M. (2007) Seasonal variations in modern speleothem calcite growth in central Texas, U.S.A.. *J. Sediment. Res.* **77**, 615–622.

Bar-Matthews M., Ayalon A., Matthews A., Sass E. and Halicz L. (1996) Carbon and oxygen isotope study of the active water–carbonate system in a karstic Mediterranean cave: implications for paleoclimate research in semiarid regions. *Geochim. Cosmochim. Acta* **60**, 337–347.

Beck J. W., Richards D. A., Edwards R. L., Silverman B. W., Smart P. L., Donahue D. J., Hererra-Osterheld S., Burr G. S., Calsoyas L., Jull A. J. T. and Biddulph D. (2001) Extremely large variations in atmospheric C-14 concentration during the last glacial period. *Science* **292**, 2453–2458.

Bowen O. E. (1973) *The Mineral Economics of the Carbonate Rocks: Limestone and Dolomite Resources of California*. California Division of Mines and Geology, Sacramento.

Capo R. C. and DePaolo D. J. (1990) Seawater strontium isotopic variations from 2.5 million years ago to the present. *Science* **249**, 51–55.

Cerling T., Solomon D. K., Quade J. and Bowman R. (1991) On the isotopic composition of carbon in soil carbon dioxide. *Geochim. Cosmochim. Acta* **55**, 3403–3405.

Cheng H., Edwards R. L., Hoff J., Gallup C. D., Richards D. A. and Asmerom Y. (2000) The half-lives of uranium-234 and thorium-230. *Chem. Geol.* **169**, 17–33.

Cheng H., Edwards R. L., Broecker W. S., Denton G. H., Kong X., Wang Y., Zhang R. and Wang X. (2009) Ice age terminations. *Science* **326**, 248–252.

Clark W. B. and Lydon P. A. (1962) *Mines and Mineral Resources of Calaveras County, California*. California Division of Mines and Geology, San Francisco.

Cole K. (1983) Late Pleistocene vegetation of Kings Canyon, Sierra Nevada, California. *Quaternary Res.* **19**, 117–129.

Cruz, Jr., F. W., Burns S. J., Karmann I., Sharp W. D., Vuille M. and Ferrari J. A. (2006) A stalagmite record of changes in atmospheric circulation and soil processes in the Brazilian subtropics during the Late Pleistocene. *Quaternary Sci. Rev.* **25**, 2749–2761.

Cruz F. W., Vuille M., Burns S. J., Wang X., Cheng H., Werner M., Edwards R. L., Karmann I., Auler A. and Nguyen H. (2009) Orbitally driven east–west antiphasing of South American precipitation. *Nat. Geosci.* **2**, 210–214.

Davidson E. A. and Janssens I. A. (2006) Temperature sensitivity of soil carbon decomposition and feedbacks to climate change. *Nature* **440**, 165–173.

Davis O. K. (1999) Pollen analysis of Tulare Lake, California: Great Basin-like vegetation in Central California during the full-glacial and early Holocene. *Rev. Palaeobot. Palynol.* **107**, 249–257.

Denniston R. F., Asmerom Y., Polyak V., Dorale J. A., Carpenter S. J., Trodick C., Hoye B. and Gonzalez L. A. (2007) Synchronous millennial-scale climatic changes in the Great Basin and the North Atlantic during the last interglacial. *Geology* **35**, 619–622.

DePaolo D. J. and Ingram B. L. (1985) High-resolution stratigraphy with strontium isotopes. *Science* **227**, 938–941.

Dorale J. A., Edwards R. L., Ito E. and Gonzalez L. A. (1998) Climate and vegetation history of the midcontinent from 75 to 25 ka: a speleothem record from Crevice Cave, Missouri, USA. *Science* **282**, 1871–1874.

Dorale J. A. and Liu Z. (2009) Limitations of hendy test criteria in judging the paleoclimatic suitability of speleothems and the need for replication. *J. Cave Karst Stud.* **71**, 73–80.

Dulinski M. and Rozanski K. (1990) Formation of $^{13}C/^{12}C$ isotope ratios in speleothems: a semi-dynamic model. *Radiocarbon* **32**, 7–16.

Edwards R. L., Chen J. H. and Wasserburg G. J. (1987) 238U–234U–230Th–232Th systematics and the precise measurement of time over the past 500,000 years. *Earth Planet. Sc. Lett.* **81**, 175–192.

Ersek V., Hostetler S. W., Cheng H., Clark P. U., Anslow F. S., Mix A. C. and Edwards R. L. (2009) Environmental influences on speleothem growth in southwestern Oregon during the last 380,000 years. *Earth Planet. Sci. Lett.* **279**, 316–325.

Fairchild I. J., Borsato A. F., Frisia S., Hawkesworth C. J., Huang Y., McDermott F. and Spiro B. (2000) Controls on trace element (Sr–Mg) compositions of carbonate cave waters: implications for speleothem climatic records. *Chem. Geol.* **166**, 255–269.

Fairchild I. J. (2006) Modification and preservation of environmental signals in speleothems. *Earth Sci. Rev.* **75**, 105–153.

Fleitmann D., Burns S. J., Mangini A., Mudelsee M., Kramers J., Villa I., Neff U., Al-Subbary A. A., Buettner A., Hippler D. and Matter A. (2007) Holocene ITCZ and Indian monsoon dynamics recorded in stalagmites from Oman and Yemen (Socotra). *Quaternary Sci. Rev.* **26**, 170–188.

Frumkin A., Ford D. C. and Schwarcz H. P. (2000) Paleoclimate and vegetation of the last glacial cycles in Jerusalem from a speleothem record. *Global Biogeochem. Cy.* **14**, 863–870.

Genty D., Massault M., Gilmour M., Baker A., Verheyden S. and Keppens E. (1999) Calculation of past dead carbon proportion and variability by the comparison of AMS ^{14}C and TIMS U/Th ages on two Holocene stalagmites. *Radiocarbon* **41**, 251–270.

Genty D., Baker A., Massault M., Proctor C., Gilmour M., Pons-Branchu E. and Hamelin B. (2001) Dead carbon in stalagmites: Carbonate bedrock paleodissolution vs. ageing of soil organic matter. Implications for ^{13}C variations in speleothems. *Geochim. Cosmochim. Acta* **65**, 3443–3457.

Genty D. and Massault M. (1999) Carbon transfer dynamics from bomb 14C and $\delta^{13}C$ time series of a laminated stalagmite from SW-France. Modelling and comparison with other stalagmite. *Geochim. Cosmochim. Acta* **63**, 1537–1548.

Genty D., Blamart D., Ouahdi R., Gilmour M., Baker A., Jouzel J. and Van-Exter S. (2003) Precise dating of Dansgaard-Oeschger climate oscillations in western Europe from stalagmite data. *Nature* **421**, 833–837.

Guilderson T. P., Southon J. R. and Brown T. A. (2003) High-precision AMS 14C results on TIRI/FIRI turbidite. *Radiocarbon* **45**, 75–80.

Hellstrom J. (2006) U–Th dating of speleothems with high initial ^{230}Th using stratigraphical constraint. *Quaternary Geochronology* **1**, 289–295.

Hendy C. H. (1971) The isotopic geochemistry of speleothems. I: The calculation of the effects of different modes of formation on the isotopic composition of speleothems and their applicability as palaeoclimatic indicators. *Geochim. Cosmochim. Acta* **35**, 801–824.

Hendy I. L., Kennett J. P., Roark E. B. and Ingram B. L. (2002) Apparent synchroneity of submillennial scale climate events between Greenland and Santa Barbara Basin, California from 30–10 ka. *Quaternary Sci. Rev.* **21**, 1167–1184.

Hoffmann D. L., Beck J. W., Richards D. A., Smart P. L., Singarayer J. S., Ketchmark T. and Hawkesworth C. J. (2010) Towards radiocarbon calibration beyond 28 ka using speleothems from the Bahamas. *Earth Planet. Sci. Lett.* **289**, 1–10.

Ingram B. L. and Lin J. C. (2002) Geochemical tracers of sediment sources to San Francisco Bay. *Geology* **30**, 575–578.

James E. W. and Banner J. L. (2008) A global model for seasonal preservation bias in speleothem proxy records. *Geol. Soc. Am. Abstr. Prog.* **40**, 166–167.

Johnson K. R., Hu C., Belshaw N. S. and Henderson G. M. (2006) Seasonal trace-element and stable-isotope variations in a Chinese speleothem: the potential for high-resolution paleo-monsoon reconstruction. *Earth Planet. Sci. Lett.* **244**, 394–407.

Ludwig K. R., Wallace A. R. and Simmons K. R. (1985) The Schwartzwalder uranium deposit. II: Age of uranium mineralization and Pb-isotope constraints on genesis. *Econ. Geol.* **80**, 1858–1871.

Ludwig K. R. and Paces J. B. (2002) Uranium-series dating of pedogenic silica and carbonate, Crater Flat, Nevada. *Geochim. Cosmochim. Acta* **66**, 487–506.

Ludwig K. R. (2003) Using Isoplot/Ex, Version 2.01: A geochronological toolkit for Microsoft Excel. Berkeley Geochronology Center Special Publication, vol. 1a, Berkeley Geochronology Center, Berkeley, California. 47p.

McDermott F. (2004) Palaeo-climate reconstruction from stable isotope variations in speleothems: a review. *Quaternary Sci. Rev.* **23**, 901–918.

Mickler P. J., Banner J. L., Stern L., Asmerom Y., Edwards R. L. and Ito E. (2004) Stable isotope variations in modern tropical speleothems: evaluating equilibrium vs. kinetic isotope effects. *Geochim. Cosmochim. Acta* **68**, 4381–4393.

Mickler P. J., Stern L. and Banner A. J. L. (2006) Large kinetic isotope effects in modern speleothems. *Geol. Soc. Am. Bull.* **118**, 65–81.

Montañez I. P., Osleger D. A., Banner J. L., Mack L. and Musgrove M. L. (2000) Evolution of the Sr annd C isotope composition of Cambrian oceans. *GSA Today* **10**, 1–5.

Neff U., Burns S. J., Mangini A., Mudelsee M., Fleitmann D. and Matter A. (2001) Strong coherence between solar variability and the monsoon in Oman between 9 and 6 kyr ago. *Nature* **411**, 290–293.

Oster J. L., Montañez I. P., Sharp W. D. and Cooper K. M. (2009) Late Pleistocene California droughts during deglaciation and Arctic warming. *Earth Planet. Sci. Lett.* **288**, 434–443.

Palmer M. R. and Edmond J. M. (1989) The strontium isotope budget of the modern ocean. *Earth Planet. Sci. Lett.* **92**, 11–26.

Partin J. W., Cobb K. M., Adkins J. F., Clark B. and Fernandez D. P. (2007) Millennial-scale trends in west Pacific warm pool hydrology since the Last Glacial Maximum. *Nature* **449**, 452–456.

Polyak V. J., Rasmussen J. B. T. and Asmerom Y. (2004) Prolonged wet period in the southwestern United States through the Younger Dryas. *Geology* **32**, 5–8.

Raich J. W. and Schlesinger W. H. (1992) The global carbon dioxide flux in soil respiration and its relationship to vegetation and climate. *Tellus* **44B**, 81–99.

Reimer P. J., Baillie M. G. L., Bard E., Bayliss A., Beck J. W., Blackwell P. G., Bronk Ramsey C., Buck C. E., Burr G. S., Edwards R. L., Friedrich M., Grootes P. M., Guilderson T. P., Hajdas I., Heaton T. J., Hogg A. G., Hughen K. A., Kaiser K. F., Kromer B., McCormac F. G., Manning S. W., Reimer R. W., Richards D. A., Southon J. R., Talamo S., Turney C. S. M., van der Plicht J. and Weyhenmeyer C. E. (2010) IntCal09 and Marine09 Radiocarbon Age Calibration Curves, 0–50,000 years cal BP. 0–26 cal kyr BP. *Radiocarbon* **51**, 1111–1150.

Romanek C. S., Grossman E. L. and Morse J. W. (1992) Carbon isotopic fractionation in synthetic aragonite and calcite- effects of temperature and precipitation rate. *Geochim. Cosmochim. Acta* **56**, 419–430.

Sarkar A., Ramesh R. and Bhattacharya S. K. (1990) Effect of sample pretreatment and size fraction on the $\delta^{18}O$ and $\delta^{13}C$ values of foraminifera in Arabian Sea sediments. *Terra Nova* **2**, 488–492.

Shakun J. D., Burns S. J., Fleitman D., Kramers J., Matter A. and Al-Subary A. (2007) A high-resolution, absolute-dated deglacial speleothem record of Indian Ocean climate from Socotra Island, Yemen. *Earth Planet. Sci. Lett.* **259**, 442–456.

Short H. W. (1975) The geology of Moaning Cave, Calaveras County, California. *Calif. Geol.* **28**, 195–201.

Stuiver M. and Polach H. A. (1977) Reporting of ^{14}C data. *Radiocarbon* **19**, 355–363.

Stuiver M. and Grootes P. M. (2000) GISP2 oxygen isotope ratios. *Quaternary Res.* **53**, 277–284.

Svensson A., Andersen K. K., Bigler M., Clausen H. B., Dahl-Jensen D., Davies S. M., Johnsen S. J., Muscheler R., Rasmussen S. O., Röthlishberger R., Steffensen J. P. and Vinther B. M. (2006) The Greenland ice core chronology 2005, 15–42 ka. Part 2: Comparison to other records. *Quaternary Sci. Rev.* **25**, 3258–3267.

Thompson R. S., Whitlock C., Bartlein P. J., Harrison S. P. and Spaulding W. G. (1993) Climatic changes in the western United States since 18,000 yr B.P. In *Global Climates since the Last Glacial Maximum* (eds. H. E. Wright Jr., J. E. Kutzbach, T. Webb III, W. F. Ruddiman, F. A. Street-Perrott and P. J. Bartlein). University of Minnesota Press, Minneapolis. 569 p.

Treble P. C., Chappell J. and Shelley J. M. G. (2005) Complex speleothem growth processes revealed by trace element mapping and scanning electron microscopy of annual layers. *Geochim. Cosmochim. Acta* **69**, 4855–4863.

Trumbore S. E. (1993) Comparison of carbon dynamics in tropical and temperate soils using radiocarbon measurements. *Global Biogeochem. Cy.* **7**, 275–290.

Vacco D. A., Clark P. U., Mix A. C., Cheng H. and Edwards R. L. (2005) A speleothem record of Younger Dryas cooling, Klamath Mountains, Oregon, USA. *Quaternary Res.* **64**, 249–256.

Verheyden S., Nader F. H., Cheng H. J., Edwards L. R. and Swennen R. (2008) Paleoclimate reconstruction in the Levant region from the geochemistry of a Holocene stalagmite from the Jeita cave, Lebanon. *Quaternary Res.* **70**, 368–381.

Vogel J. S., Southon J. R. and Nelson D. E. (1987) Catalyst and binder effects in the use of filamentous graphite for AMS. *Nucl. Instrum. Methods B.* **29**, 50–56.

Wagner J. D. M., Cole J. E., Beck J. W., Patchett P. J., Henderson G. M. and Barnett H. R. (2010) Moisture variability in the southwestern United States linked to abrupt glacial climate change. *Nat. Geosci.* **3**, 110–113.

Wang Y. J., Cheng H., Edwards R. L., An Z. S., Wu J. Y., Shen C.-C. and Dorale J. A. (2001) A high-resolution absolute-dated Late Pleistocene monsoon record from Hulu Cave, China. *Science* **294**, 2345–2348.

Wang Y., Cheng H., Edwards R. L., He Y., Kong X., An Z., Wu J., Kelly M. J., Dykoski C. A. and Li X. (2005) The Holocene Asian Monsoon: links to solar changes and North Atlantic climate. *Science* **308**, 854–857.

Zhang J., Quay P. D. and Wilbur D. O. (1995) Carbon-isotope fractionation during gas–water exchange and dissolution of CO_2. *Geochim. Cosmochim. Acta* **59**, 107–114.

Associate editor: Miryam Bar-Matthews